

BBA 41541

ELECTRON TRANSFER IN REACTION CENTERS OF *RHODOPSEUDOMONAS SPHAEROIDES*I. DETERMINATION OF THE CHARGE RECOMBINATION PATHWAY OF $D^+Q_AQ_B^-$ AND FREE ENERGY AND KINETIC RELATIONS BETWEEN $Q_A^-Q_B$ AND $Q_AQ_B^-$

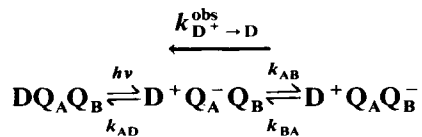
D. KLEINFELD *, M.Y. OKAMURA and G. FEHER **

Department of Physics, University of California at San Diego, La Jolla, CA 92093 (U.S.A.)

(Received October 31st, 1983)

Key words: Bacterial photosynthesis; Reaction center; Electron transfer; Charge recombination; (*R. sphaeroides*)

The electron-transfer reactions and thermodynamic equilibria involving the quinone acceptor complex in bacterial reaction centers from *R. sphaeroides* were investigated. The reactions are described by the scheme:



We found that the charge recombination pathway of $D^+Q_AQ_B^-$ proceeds via the intermediate state $D^+Q_A^-Q_B$, the direct pathway contributing less than approx. 5% to the observed recombination rate. The method used to obtain this result was based on a comparison of the kinetics predicted for the indirect pathway (given by the product k_{AD} -times the fraction of reaction centers in the $Q_A^-Q_B$ state) with the observed recombination rate, $k_{D^+ \rightarrow D}^{obs}$. The kinetic measurements were used to obtain the pH dependence ($6.1 \leq \text{pH} \leq 11.7$) of the free energy difference between the states $Q_A^-Q_B$ and $Q_AQ_B^-$. At low pH (less than 9) $Q_AQ_B^-$ is stabilized relative to $Q_A^-Q_B$ by 67 meV, whereas at high pH $Q_A^-Q_B$ is energetically favored. Both Q_A^- and Q_B^- associate with a proton, with pK values of 9.8 and 11.3, respectively. The stronger interaction of the proton with Q_B^- provides the driving force for the forward electron transfer.

Introduction

Reaction centers from photosynthetic bacteria are membrane-bound protein-pigment complexes that act as energy transducers, absorbing light and

converting it to electrochemical energy through the creation of oxidized and reduced molecules. The reaction center consists of three polypeptides and a number of cofactors associated with the electron transfer chain: four bacteriochlorophylls, two bacteriopheophytins, one nonheme iron (Fe^{2+}) and two ubiquinones (UQ-10) (for review, see Ref. 1). The energy conversion entails a light-induced charge separation that is stabilized for progressively longer times as the electron passes serially through the electron-acceptor chain (for review, see Ref. 2). The temporal stabilization requires a

* Work performed in partial fulfillment for the Ph. D. degree.

** To whom reprint requests should be addressed.

Abbreviations: LDAO, lauryldimethylamine *N*-oxide; Mes, 4-morpholineethanesulfonic acid; Pipes, 1,4-piperazineethanesulfonic acid; Ches, cyclohexylaminoethanesulfonic acid; Caps, 3-(cyclohexylamino)propanesulfonic acid.

concomitant decrease in the free energy of the system after each transfer step.

In this work we focus on a subsystem of the charge separation process as illustrated in Fig. 1. This subsystem consists of the primary electron donor, D (a bacteriochlorophyll dimer), and the two quinone acceptors, Q_A and Q_B . The charge recombination of the state $D^+Q_AQ_B^-$ can proceed either directly, with rate k_{BD} , or indirectly via the intermediate state, $D^+Q_A^-Q_B$. The determination of the charge recombination pathway has been discussed by a number of authors [3–5], who had obtained conflicting results. In this paper, we describe the determination of the dominant pathway by a method that, unlike previous ones, is relatively insensitive to systematic errors.

The charge recombination is monitored via the observed donor recovery rate, $k_{D^+ \rightarrow D}^{\text{obs}}$, which can be expressed as the sum of a direct and indirect pathway (see Appendix). The contribution of the indirect pathway is given by the product of the charge recombination rate, k_{AD} , and the fraction, α , of reaction centers in the state $Q_A^-Q_B$ (i.e., $k_{\text{indirect}} = \alpha k_{AD}$). The basis of our method to determine the pathway is to measure both α and k_{AD} , and to compare the product of these quanti-

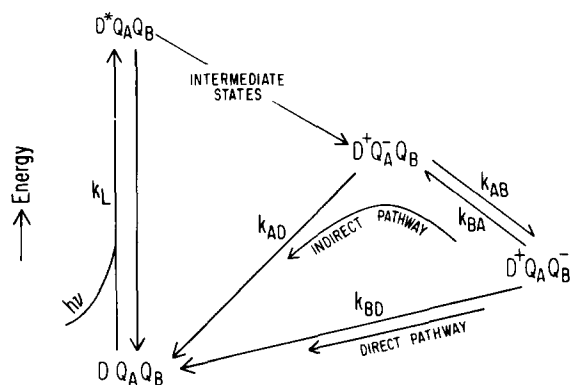


Fig. 1. Simplified electron transfer scheme in reaction centers involving the donor (D) and the primary and secondary quinone acceptors, Q_A and Q_B (energy axis not to scale). Absorption of light causes an electron to leave D to form $D^+Q_AQ_B^-$ after passing through a number of intermediate states. The electron on Q_B^- can recombine with the hole on D^+ either directly, with rate k_{BD} , or indirectly with $D^+Q_A^-Q_B$ serving as the intermediate state. The observed charge-recombination rate is given by Eqn. 3. The states $D^+Q_A^-Q_B$ and $D^+Q_AQ_B^-$ are shown for simplicity unprotonated; at $\text{pH} < 9$ they both associate with a proton as discussed later in the text.

ties with $k_{D^+ \rightarrow D}^{\text{obs}}$. If the product αk_{AD} equals $k_{D^+ \rightarrow D}^{\text{obs}}$, the charge recombination proceeds via the indirect pathway. If a discrepancy between the values $k_{D^+ \rightarrow D}^{\text{obs}}$ and αk_{AD} is found, the contribution of the direct recombination rate k_{BD} can be obtained.

The rate $k_{D^+ \rightarrow D}^{\text{obs}}$ was measured by monitoring flash induced optical absorption changes at 865 nm. When the electron transfer from Q_A^- to Q_B was blocked, this measurement determined k_{AD} . The electron transfer rate between $Q_A^-Q_B$ and $Q_AQ_B^-$, given by $k_{AB} + k_{BA}$, was determined from the rate of decay of Q_A^- after a flash. The fraction, α , of reaction centers in the state $Q_A^-Q_B$ was obtained by measuring the amount of cytochrome *c* oxidized by D^+ after successive flashes. All kinetics were investigated at several pH values. This allowed us to establish the charge recombination pathway over a wide pH range.

Once the charge recombination pathway was determined, the kinetic measurements presented in this study were used to obtain the pH dependence of the free energy difference (ΔG_{obs}^0) between the states $Q_A^-Q_B$ and $Q_AQ_B^-$. This dependence was used to model the role of protonation in the stabilization of Q_A^- and Q_B^- . From the pH dependence of ΔG_{obs}^0 , the $\text{p}K_{A^-}$ and $\text{p}K_{B^-}$ values associated with the protonation of $Q_A^-Q_B$ and $Q_AQ_B^-$ were determined and compared with the values obtained from redox titration measurements [6–8]. Similarly, the pH dependences of the individual electron transfer rates k_{AB} and k_{BA} were deduced.

Preliminary accounts of this work have been presented [9,10]. In a forthcoming paper (no. II in this series), we will examine the charge recombination pathway of the state $D^+Q_AQ_B^{2-}$ and free energy and kinetic relations between the states $Q_A^-Q_B^-$ and $Q_AQ_B^{2-}$.

Materials and Methods

Reagents

Horse heart cytochrome *c* (cyt *c*) was obtained from Sigma (type III). Cytochrome c_2 was purified from *R. sphaeroides* R-26 by the method of Bartsch [11]. Both cytochromes were reduced by sodium dithionite (Matheson, Coleman and Bell), purified on a Sephadex G-200 gel filtration column (Pharmacia Fine Chemicals) and stored in 10 mM

Tris (pH 8.0). Solutions of 1,10-phenanthroline (*o*-phen; Baker) and UQ-10 (Sigma) were prepared in ethanol prior to use.

Reaction centers

Reaction centers were isolated from *Rhodospseudomonas sphaeroides* R-26 as described [1]. To avoid damaging the Q_B binding site, the concentration of lauryldimethylamine *N*-oxide (LDAO; Onyx) was kept at or below 0.1% (w/v) after the extraction of the reaction centers from the cell membrane. Reaction centers containing one quinone or less were prepared by the method of Okamura et al. [12]. The ubiquinone content for each preparation was determined by two different assays. A cytochrome *c* photooxidation assay measured the number of quinones through the total number of electrons transferred to the quinone acceptors [13,14]. A second assay measured the kinetics of the $D^+ \rightarrow D$ transition, which was decomposed into 'fast' and 'slow' components, the latter indicating a functional Q_B [14].

For experiments with reaction centers in the presence of excess ubiquinone, solid UQ-10 was dispersed in the buffer solution by vortexing for approx. 5 min. This was followed by sonication for 5 min, at the end of which the reaction centers were added.

Buffers

All experiments were carried out in 10 mM buffer and 0.025% (w/v) LDAO with potassium chloride added as required to set the ionic strength at 10 mM. The following pH buffers were used: 4-morpholineethanesulfonic acid (Mes; Calbiochem-Behring), below pH 6.7; 1,4-piperazine-diethanesulfonic acid (Pipes; Sigma), pH 6.7–7.7; 2-amino-2-hydroxymethylpropane-1,3-diol (Tris; Schwarz/Mann), pH 7.7–9.0; cyclohexylaminoethanesulfonic acid (Ches; Calbiochem-Behring), pH 9.0–10.2; and 3-(cyclohexylamino)propanesulfonic acid (Caps; Calbiochem-Behring), above pH 10.0.

Optical measurements

The kinetics of the optical absorbance changes were monitored with a single beam spectrophotometer modified from an earlier design [15]; it had a time resolution of 0.5 μ s. Sample cuvettes were held in a thermostated jacket kept at 21.5 °C.

The monitoring beam was detected with a Hamamatsu R-666S photomultiplier tube and the output, after amplification and filtering, was recorded on a digital oscilloscope (Nicolet Instruments 1090A). The data were analyzed and stored using a Z-80 microprocessor based computer system of local design, which also controlled the digital oscilloscope for signal averaging. First-order rate constants were determined graphically by fitting the logarithm of the absorbance change with a straight line. The baseline was established from the level of absorbance after the change had decayed to within the noise level. The actinic flashes, approx. 0.4 μ s in duration, were provided by a dye laser (Phase-R Corporation DL-2100C) with either Rhodamine 610 dye dissolved in ethanol or Rhodamine 590 dye dissolved in methanol. Flash energy, measured with a thermopile (Konrad Laser System model 101), was typically 0.2 J. Care was taken to ensure that the volume of reaction centers interrogated by the monitoring beam was kept smaller than the volume excited by the laser flash.

pH measurements

pH measurements were performed with a Radiometer RPHM64 research pH meter and GK2401-B electrode calibrated with buffer standards at the two closest integer pH values spanning the measured pH. Measurements were performed on samples immediately before or after data were acquired. Corrections were made for small pH changes due to temperature differences ($|\Delta T| < 3^\circ\text{C}$) between the time of data acquisition and the time of pH measurements.

Theoretical models

Electron transfer rates after a single flash

After the termination of the laser flash, the reaction centers are in the charge-separated state $D^+ Q_A^- Q_B$. The kinetics governing the subsequent electron transfers are determined by an algebraic combination of the transition rates, k_{AD} , k_{BD} , k_{AB} and k_{BA} , between the various states (see Fig. 1).

When the electron transfer rate between the states $^* Q_A^- Q_B$ and $Q_A Q_B^-$ is fast compared with

* For simplicity, the various reaction center states are written unprotonated. However, they are meant to include the protonated states as well. The topic of protonation is discussed in a later section.

the charge recombination of either Q_A^- or Q_B^- with D^+ , i.e.:

$$k_{AB} + k_{BA} \gg k_{AD} \quad \text{and} \quad k_{AB} + k_{BA} \gg k_{BD} \quad (1)$$

the electron on Q_A^- passes to Q_B before recombining with D^+ . In this approximation, the electron transfer rate for $Q_A^-Q_B \rightleftharpoons Q_AQ_B^-$ is given by the observed decay rate of Q_A^- or formation rate of Q_B^- (see Appendix, Eqn. A-5), i.e.:

$$k_{Q_A^- \rightarrow Q_A}^{\text{obs}} = k_{Q_B^- \rightarrow Q_B}^{\text{obs}} = k_{AB} + k_{BA} \quad (2)$$

The recombination rate of an electron on Q_A^- or Q_B^- with D^+ can be monitored via the donor recovery rate $k_{D^+ \rightarrow D}^{\text{obs}}$. In the approximation of Eqn. 1, this rate can be expressed as the sum of an indirect and a direct pathway (see Appendix, Eqn. A-7), i.e.:

$$k_{D^+ \rightarrow D}^{\text{obs}} = k_{\text{indirect}} + k_{\text{direct}} = \alpha k_{AD} + (1 - \alpha) k_{BD} \quad (3)$$

The partition coefficient, α , is the fraction of reaction centers in the state $Q_A^-Q_B$ and is given by:

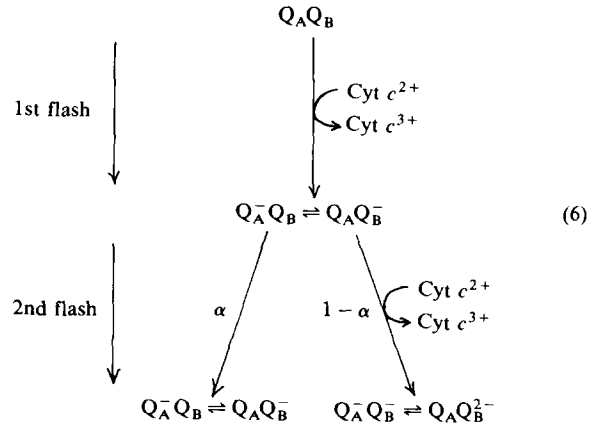
$$\alpha = \frac{[Q_A^-Q_B]}{[Q_A^-Q_B] + [Q_AQ_B^-]} = \frac{k_{BA}}{k_{AB} + k_{BA}} \quad (4)$$

In reaction centers in which the electron transfer from Q_A^- to Q_B is blocked or in reaction centers with one quinone, $\alpha = 1$, and:

$$k_{D^+ \rightarrow D}^{\text{obs}} = k_{Q_A^- \rightarrow Q_A}^{\text{obs}} = k_{AD} \quad (5)$$

Distribution of reaction center states after successive flashes

In the presence of an exogenous electron donor (e.g., $\text{cyt } c^{2+}$), D^+ is reduced and the electron is trapped on the quinone acceptors following the light-induced charge separation. With successive flashes electrons are added to the quinones as long as Q_A is unreduced [16,17]; reaction centers in the state DQ_A^- are photochemically inactive on the time scale of the reaction with $\text{cyt } c^{2+}$. The mixture of states present after the first two flashes are shown below:



The equilibrium partitioning between the states $Q_A^-Q_B$ and $Q_AQ_B^-$ is described by the partition coefficient α (see Eqn. 4). The equilibrium partitioning between the two electron states, $Q_A^-Q_B$ and $Q_AQ_B^{2-}$, is relevant for determining the distribution of RC states after the second flash [10].

The value of α was obtained by measuring the amount of cytochrome oxidized after the first and second flash. Cytochrome oxidation was monitored optically at 550 nm. The absorption change after the first flash (ΔA_1^{550}) corresponds to one $\text{cyt } c^{2+}$ per reaction center, while the absorption change after the second flash (ΔA_2^{550}) corresponds to $(1 - \alpha)$ $\text{cyt } c^{2+}$ oxidized per reaction center. Thus, α is determined from:

$$\alpha = \frac{\Delta A_1^{550} - \Delta A_2^{550}}{\Delta A_1^{550}} \quad (7)$$

For Eqn. 7 to hold, all reaction centers must contain exactly two quinones. If the average number of quinones is less than 2.0 but greater than 1.0, one $\text{cyt } c^{2+}$ per reaction center is still oxidized on the first flash, while on the second and successive flashes the $\text{cyt } c^{2+}$ oxidation is controlled by the fraction of reaction centers with two quinones. Defining δ as the fraction of reaction centers with one quinone, Eqn. 7 is modified and becomes:

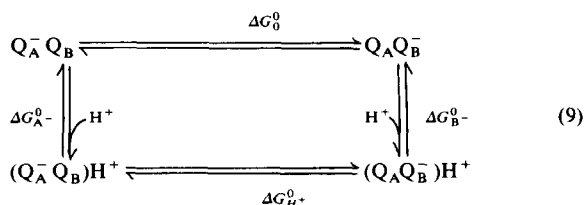
$$\alpha = \frac{(1 - \delta)\Delta A_1^{550} - \Delta A_2^{550}}{(1 - \delta)\Delta A_1^{550}} \quad (8)$$

In the above analysis it was implicitly assumed that the intermediate state $D^+I^-Q_A$ (omitted from Fig. 1) does not oxidize $\text{cyt } c^{2+}$. This assumption

is well satisfied, since the recombination time of the intermediate acceptor I^- with D^+ is much faster (approx. 10^{-8} s) [18] than either the oxidation of cyt c^{2+} by D^+ (faster than 10^{-6} s) [19–21, 48] or the electron transfer time from Q_A^- to Q_B or Q_B^- (faster than 10^{-4} s) [22–24]. Thus $D^+I^-Q_A$ does not live long enough to react with cyt c^{2+} .

Thermodynamic model for the pH dependence of free energies

The kinetic assays discussed in the previous sections do not distinguish between protonated and unprotonated species. To examine the role of protonation, the reactions were modeled by the following simple equilibrium scheme:



The standard free energies are defined and related to the acid dissociation constants pK_{A^-} and pK_{B^-} by the following relations:

$$\Delta G_0^0 \equiv G_{Q_A Q_B^-}^0 - G_{Q_A^- Q_B}^0 = -kT \ln \frac{[Q_A Q_B^-]}{[Q_A^- Q_B]} \quad (10a)$$

$$\begin{aligned}
 \Delta G_{H^+}^0 &\equiv G_{(Q_A Q_B^-)H^+}^0 - G_{(Q_A^- Q_B)H^+}^0 \\
 &= -kT \ln \frac{[(Q_A Q_B^-)H^+]}{[(Q_A^- Q_B)H^+]} \quad (10b)
 \end{aligned}$$

$$\begin{aligned}
 \Delta G_B^0 &\equiv G_{(Q_A Q_B^-)H^+}^0 - G_{Q_A Q_B^-}^0 \\
 &= -kT \ln \frac{[(Q_A Q_B^-)H^+]}{[Q_A Q_B^-]} = -kT \cdot \ln 10 \cdot (pK_{B^-} - pH) \quad (10c)
 \end{aligned}$$

$$\begin{aligned}
 \Delta G_A^0 &\equiv G_{(Q_A^- Q_B)H^+}^0 - G_{Q_A^- Q_B}^0 \\
 &= -kT \ln \frac{[(Q_A^- Q_B)H^+]}{[Q_A^- Q_B]} = -kT \cdot \ln 10 \cdot (pK_{A^-} - pH) \quad (10d)
 \end{aligned}$$

where k is Boltzmann's constant and T is the

absolute temperature. From energy conservation, the sum of all ΔG^0 's is zero, i.e.:

$$\Delta G_0^0 - \Delta G_{H^+}^0 - kT \cdot \ln 10 \cdot (pK_{B^-} - pK_{A^-}) = 0 \quad (11)$$

The measured free energy, ΔG_{obs}^0 , between $Q_A^- Q_B$ and $Q_A Q_B^-$ involves both the protonated and unprotonated species and is given by:

$$\Delta G_{obs}^0 = -kT \ln \frac{[Q_A Q_B^-] + [(Q_A Q_B^-)H^+]}{[Q_A^- Q_B] + [(Q_A^- Q_B)H^+]} \quad (12)$$

Substituting from Eqn. 10b–d and rearranging give:

$$\Delta G_{obs}^0 = \Delta G_{H^+}^0 - kT \ln \frac{1 + 10^{pH - pK_{B^-}}}{1 + 10^{pH - pK_{A^-}}} \quad (13)$$

Eqn. 13 describes an S-shaped curve with turning points at pK_{A^-} and pK_{B^-} . The limiting free energies at low and high pH are given by $\Delta G_{H^+}^0$ and ΔG_0^0 , respectively. Note that ΔG_{obs}^0 does not depend on the state of protonation of the neutral, initial state, $Q_A Q_B$.

Experimental results

The donor recovery rate, $k_{D^+ \rightarrow D}^{obs}$

The absorption peak at 865 nm is bleached after a laser flash as a result of the oxidation of the donor [25]. The recovery of this bleaching was used to measure the charge recombination rate, $k_{D^+ \rightarrow D}^{obs}$, between D^+ and $Q_A^- Q_B$ or $Q_A Q_B^-$. Fig. 2a shows representative data taken at two pH values (7.04 and 10.52). The kinetics were decomposed into a slow and fast component (Fig. 2b). The slow component, which contributed 90% to the total amplitude, is characteristic of reaction centers having two quinones and corresponds to the charge recombination between D^+ and $Q_A Q_B^-$. The remaining (10%) fast component, with rate approx. 10 s^{-1} , is indicative of the charge recombination between D^+ and Q_A^- . Since Q_A binds much more strongly than Q_B (Refs. 12 and 14; see also next section), this result implies that 90% of the reaction centers contained two quinones, while 10% contained one quinone.

The pH dependence of the donor recovery rate is shown in Fig. 2c. Data acquisition at the high pH range (pH 11.7) was limited by the stability of

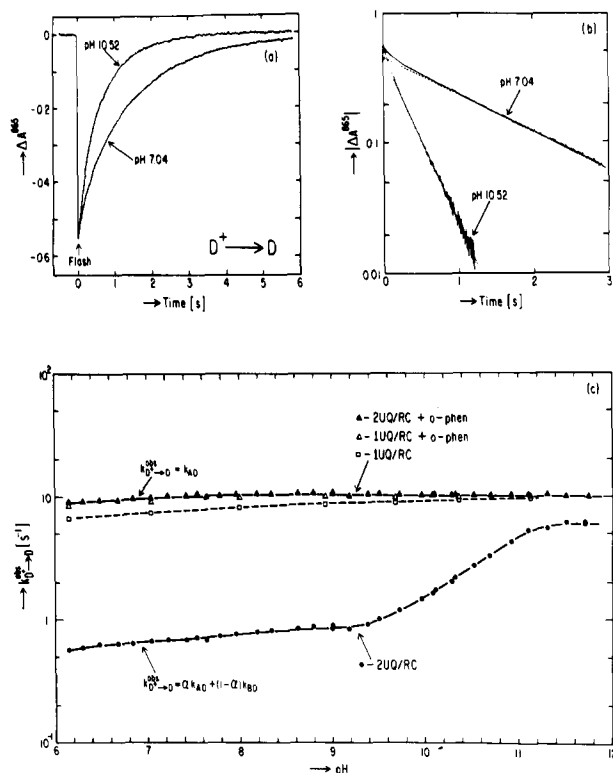


Fig. 2. (a) Optical kinetics assay of the donor recovery rate, $k_{D^+ \rightarrow D}^{obs}$, at two pH values. Conditions for pH 7.04: $5.5 \mu\text{M}$ reaction centers in 10 mM Pipes/6.2 mM KCl/0.025% LDAO; for pH 10.52: 10 mM Caps/5.5 mM KCl/0.025% LDAO, both at $T = 21.5^\circ\text{C}$. (b) Semi-logarithmic plot of the absorption changes shown in part a. The dashed lines represent the recovery rates 0.675 s^{-1} (pH 7.04) and 2.75 s^{-1} (pH 10.52). When 10 mM *o*-phen was added, the donor recovery rates changed to 9.8 s^{-1} (pH 7.04) and 10.2 s^{-1} (pH 10.52) (data not shown). (c) The pH dependence of the donor recovery rate. Conditions as in part (a) except for varying buffers. \bullet — \bullet , reaction centers averaging 1.9 quinones; recovery rate (slow component) determines $k_{D^+ \rightarrow D}^{obs}$. \blacktriangle — \blacktriangle , the same reaction center samples with 10 mM *o*-phen added; recovery rate determines k_{AD} . \square — \square , reaction centers averaging 0.76 quinones. \triangle — \triangle , the same reaction center samples with 10 mM *o*-phen added. The lines represent the best smooth fit to the data.

reaction centers. To check whether the kinetics at the highest pH values were affected by a partial (irreversible) denaturation of reaction centers, the pH of the samples was decreased after the high pH measurements and the kinetics were remeasured. Complete reversibility was observed.

Fig. 2c shows a striking difference in the pH dependence of the charge recombination rate between Q_A^- and D^+ and Q_B^- and D^+ . The latter

shows an increase in rate by nearly an order of magnitude between pH 9 and 11, whereas the $D^+Q_A^-$ recombination rate, k_{AD} , is virtually pH independent.

The $D^+Q_A^-$ recombination rate was measured in reaction centers with one quinone* (Fig. 2c, \square — \square) as well as in reaction centers with two quinones to which 10 mM *o*-phen was added to block the electron transfer from Q_A^- to Q_B^- (Fig. 2c, \blacktriangle — \blacktriangle). The results obtained from different samples were very similar, with small differences occurring towards the lower pH values. Interestingly, when *o*-phen was added to the one quinone reaction centers (Fig. 2c, \triangle — \triangle) the differences were eliminated.

The $Q_A^-Q_B^- \rightleftharpoons Q_AQ_B^-$ electron-transfer rate, $k_{Q_A^- \rightarrow Q_A}^{obs}$

The electron transfer rate between $Q_A^-Q_B^-$ and $Q_AQ_B^-$ was determined by monitoring flash-induced changes in the optical absorption spectrum at 747 nm. At this wavelength the absorption changes reflect electrochromic shifts due primarily to the presence of $Q_A^-Q_B^-$ [22]; contributions from the $D^+ \rightarrow D$ transitions are essentially absent at this wavelength.

Fig. 3a shows representative data for the flash-induced optical absorption changes at 747 nm. The rate $k_{Q_A^- \rightarrow Q_A}^{obs}$ was determined from the slope of a straight line fit to the logarithm of the absorbance change, as shown in Fig. 3b.

The pH dependence of $k_{Q_A^- \rightarrow Q_A}^{obs}$ is shown in Fig. 3c. The rate is essentially constant at $7 \cdot 10^3 \text{ s}^{-1}$ at low pH and decreases sharply when the pH is higher than approx. 9. Over the entire pH range, $k_{Q_A^- \rightarrow Q_A}^{obs}$ is at least 15-times larger than $k_{D^+ \rightarrow D}^{obs}$ (see Fig. 2c), fulfilling the condition (Eqn. 1) that led to Eqns. 2 and 3.

The effect of excess UQ-10 on $k_{Q_A^- \rightarrow Q_A}^{obs}$ was checked at pH 8.5. Using $6.0 \mu\text{M}$ reaction centers in 10 mM Tris with 12–60 μM UQ-10, no significant changes were found. Increasing the LDAO concentration to 0.05% produced no significant change, while increasing the ionic strength to 110 mM with either NaCl or KCl decreased $k_{Q_A^- \rightarrow Q_A}^{obs}$ by approx. 50%.

* To reduce the population of reaction centers with two quinones, we used a sample that had on the average only 0.76 UQ per reaction center.

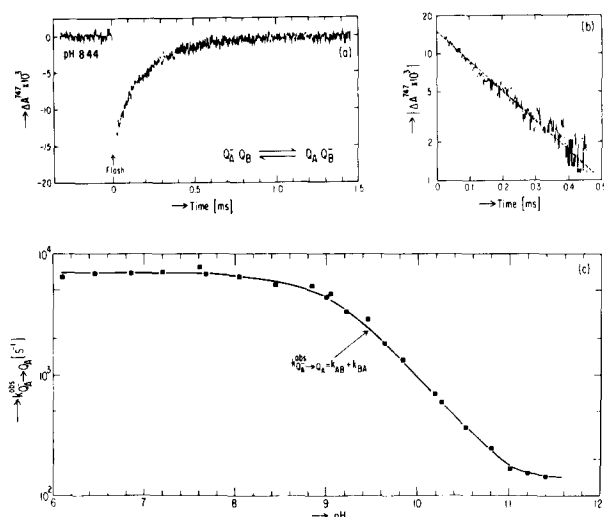


Fig. 3. (a) Optical kinetics assay for the $Q_A^- Q_B \rightleftharpoons Q_A Q_B^-$ electron transfer rate $k_{Q_A^- Q_B}^{obs}$. Conditions: $5.5 \mu\text{M}$ reaction centers in 10 mM Tris/ 5.6 mM KCl/ 0.025% LDAO (pH 8.44) $T = 21.5^\circ\text{C}$. 16 traces were averaged, with flashes at 15 s intervals. The initial spike was caused by saturation of the detector electronics, which recovered completely within $20 \mu\text{s}$. (b) Semilogarithmic plot of the absorption change shown in part (a). The dashed line represents the decay rate $5.45 \cdot 10^3 \text{ s}^{-1}$. When 10 mM *o*-phen was added to the sample, the absorbance change decayed with a rate of 10 s^{-1} (i.e., k_{AD}) (data not shown). (c) The pH dependence of $k_{Q_A^- Q_B}^{obs}$. Conditions as in part (a) except for varying buffers. Each point represents the average of 4–16 traces. Solid line represents the best smooth fit to the data.

The partition coefficient α

The relative change in cyt-*c* oxidation after successive flashes served as an assay for the partition coefficients (see Eqns. 6–8). The experimental results of the cytochrome oxidation at a particular pH value (10.15) are shown in Fig. 4a. To ensure single electron turnovers, the flashes were short (pulse width, approx. $4 \cdot 10^{-7} \text{ s}$) compared to $(k_{Q_A^- Q_B}^{obs})^{-1}$. The partition coefficient, α , was computed from the absorption changes at 550 nm after the first and second flashes by using Eqn. 8. The value of the correction factor, δ , was obtained by measuring the fraction (i.e., $1 - \delta$) of reaction centers having a functional Q_B . Two independent assays were used (see Materials and Methods section); the decomposition of the donor recovery rate gave a value of 0.90 ± 0.05 and the cytochrome-*c* photooxidation assay gave 0.98 ± 0.04 for $1 - \delta$. From the average of these two de-

terminations (0.94), a value of $\delta = 0.06$ was deduced.

The pH dependence of α is shown in Fig. 4b. Below pH 9, α has essentially a constant value of 0.07. Above pH 9, α increases monotonically with increasing pH. The effect of δ is essentially to lower uniformly the entire curve of α versus pH. The solid line in Fig. 4b represents a theoretical fit obtained from the thermodynamic model to be discussed later.

The method of determining α requires that several conditions be satisfied. To check whether this is the case, a number of control experiments described next were performed. Unless otherwise specified, they were done at pH 8.0.

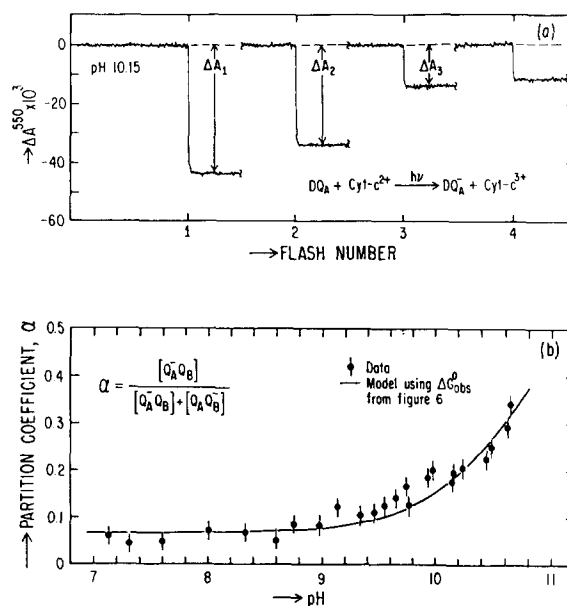


Fig. 4. Determination of the partition coefficient, α , from the cytochrome oxidation after multiple flashes. (a) Optical absorbance changes at pH 10.15. The baseline between flashes was displaced to facilitate the comparison of amplitudes. The monitoring beam was gated shut until 0.75 s before the first flash. Duration of flash, approx. $0.4 \mu\text{s}$; time between flashes, 0.6 s . The value of α was determined from ΔA_1 and ΔA_2 (see Eqn. 8) with $\delta = 0.06$. ΔA_3 can be used to determine the equilibrium between $Q_A^- Q_B^-$ and $Q_A Q_B^{2-}$ [10]. Conditions: $2.2 \mu\text{M}$ reaction centers, $20 \mu\text{M}$ cyt c^{2+} , 10 mM Caps, 3.7 mM KCl, 0.025% LDAO, $T = 21.6^\circ\text{C}$. (b) The pH dependence of α . Conditions same as in part (a), except for varying buffers. Error bars represent statistical errors (S.D. of the mean, six determinations per point). The solid line was obtained from the equilibrium data given by Eqn. 14.

The oxidation of $\text{cyt } c^{2+}$ by D^+ must be fast compared to the charge recombination of Q_B^- with D^+ . To check this condition we measured the rate of $\text{cyt } c$ oxidation, k_{cyt} , over the entire pH range. Below pH 9, the rate was pH independent, having a value of $k_{\text{cyt}} \approx 10^3 \text{ s}^{-1}$ ($[\text{cyt } c^{2+}] = 20 \mu\text{M}$, [reaction center] = $2.1 \mu\text{M}$). Above pH 9, the rate decreased sharply, limiting the assay to $\text{pH} < 10.6$, where $k_{\text{cyt}} \approx 10^2 \text{ s}^{-1}$, or approx. 30-times larger than $k_{\text{D}^+ \rightarrow \text{D}}^{\text{obs}}$ (see Fig. 2c). Cytochrome c_2 (*R. sphaeroides*) exhibited the same pH dependence as $\text{cyt } c$ and could not, therefore, be used to extend the useful pH range.

To test whether the build-up of oxidized cytochrome after successive flashes interfered with the oxidation of $\text{cyt } c^{2+}$ by D^+ , the assay was performed with varying initial concentrations of $\text{cyt } c^{2+}$. With concentrations ranging between 2- and 9-times the reaction center concentration, the measured value of α was unaffected.

To check whether electrons leak from Q_B^- between flashes or whether reactants (reaction centers or $\text{cyt } c$) are entering or leaving the monitoring volume between flashes, the time interval between laser pulses was varied from 0.35 to 2.0 s. No differences in the results were found.

An independent check on whether reaction centers enter the monitoring volume between flashes was performed with reaction centers averaging 0.76 UQ per reaction center. It was found that after the first laser flash less than 3% additional cytochromes were oxidized over the next four flashes. This residual oxidation is likely to be due to a small fraction of reaction centers with two quinones and implies that the binding constant of Q_A is at least 40-times larger than that of Q_B .

Comparison of $k_{\text{D}^+ \rightarrow \text{D}}^{\text{obs}}$ with αk_{AD}

We shall use the data presented previously to determine whether or not the charge recombination rate of $\text{D}^+ \text{Q}_A \text{Q}_B^-$ is adequately described by the indirect pathway, whose contribution to the observed rate is αk_{AD} (see Eqn. 3).

The product of α , determined from the multiple flash experiment (Fig. 4b), and k_{AD} , obtained from the donor kinetics in the presence of *o*-phen (Fig. 2c), is compared with $k_{\text{D}^+ \rightarrow \text{D}}^{\text{obs}}$ (Fig. 2c) in Fig. 5. The values of $k_{\text{D}^+ \rightarrow \text{D}}^{\text{obs}}$ and αk_{AD} appear in good numerical agreement over the entire pH range

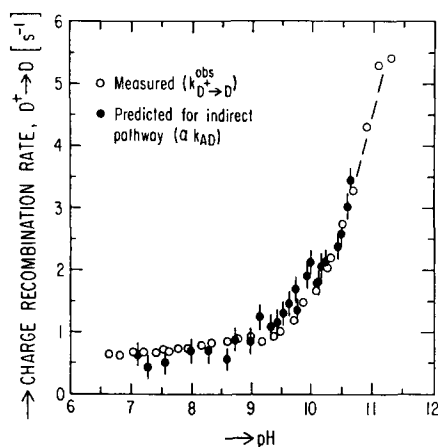


Fig. 5. Comparison between the measured charge recombination rate, $k_{\text{D}^+ \rightarrow \text{D}}^{\text{obs}}$, and the product αk_{AD} at different pH values. The product αk_{AD} was constructed by multiplying each experimental value of α (Fig. 4b) by k_{AD} taken from the smooth curve passing through the kinetics data for 2UQ/RC + *o*-phen (Fig. 2c). Error bars reflect the uncertainty in the determination of α . The close numerical agreement between $k_{\text{D}^+ \rightarrow \text{D}}^{\text{obs}}$ and αk_{AD} shows that the indirect pathway of the $\text{D}^+ \text{Q}_A \text{Q}_B^-$ charge recombination dominates.

tested. Of particular significance is the match at high pH, where the fractional error in α is smaller. Thus, the indirect charge combination pathway dominates the donor recovery kinetics.

A limit on the direct recombination rate, k_{BD} , was obtained by performing the following error analysis: a constant value of k_{BD} was chosen to minimize the mean square error between $k_{\text{D}^+ \rightarrow \text{D}}^{\text{obs}}$ and $\alpha k_{\text{AD}} + (1 - \alpha)k_{\text{BD}}$. The data obtained over the full pH range resulted in a value $k_{\text{BD}} = -0.1 \pm 0.3 \text{ s}^{-1}$, implying that $k_{\text{BD}} \leq 0.2 \text{ s}^{-1}$. By restricting the error analysis to the high pH data ($\text{pH} > 10$), a value of $k_{\text{BD}} \leq 0.1 \text{ s}^{-1}$ was obtained. This corresponds to a contribution of less than 5% to $k_{\text{D}^+ \rightarrow \text{D}}^{\text{obs}}$ via the direct pathway.

The pH dependence of the free energy between $\text{Q}_A \text{Q}_B^-$ and $\text{Q}_A^- \text{Q}_B$

When the charge recombination of $\text{D}^+ \text{Q}_A \text{Q}_B^-$ occurs via the indirect pathway, the free energy difference, ΔG_{obs}^0 , between the states $\text{Q}_A \text{Q}_B^-$ and $\text{Q}_A^- \text{Q}_B$ (see footnote in the Theoretical Models section) can be obtained from Eqn. 3 by setting $k_{\text{BD}} = 0$ and rewriting Eqn. 12 in terms of the

observed quantities; i.e.:

$$\Delta G_{\text{obs}}^0 = -kT \ln \frac{1-\alpha}{\alpha} = -kT \ln \frac{k_{\text{AD}} - k_{\text{D}^+ \rightarrow \text{D}}^{\text{obs}}}{k_{\text{D}^+ \rightarrow \text{D}}^{\text{obs}}} \quad (14)$$

The kinetics data of Fig. 2c (2UQ per reaction center with and without *o*-phen) were used to construct the pH dependence of ΔG_{obs}^0 , as shown in Fig. 6. The solid line represents a best fit to the theoretical expression given by Eqn. 13 with $\text{p}K_{\text{A}^-}$ and $\text{p}K_{\text{B}^-}$ as adjustable parameters. The results show that $\text{Q}_\text{A}^- \text{Q}_\text{B}$ favors protonation below pH 9.8 ($\text{p}K_{\text{A}^-}$), whereas $\text{Q}_\text{A} \text{Q}_\text{B}^-$ favors protonation below pH 11.3 ($\text{p}K_{\text{B}^-}$). Also shown in Fig. 6 is the poor fit obtained if one assumes that $\text{Q}_\text{A} \text{Q}_\text{B}^-$ is always protonated ($\text{p}K_{\text{B}^-} \rightarrow \infty$). The constant value of ΔG_{obs}^0 found at low pH correspond to the free-energy difference between the protonated states ($\Delta G_{\text{H}^+}^0 = -67$ meV) with $(\text{Q}_\text{A} \text{Q}_\text{B}^-) \text{H}^+$ being favored. At high pH, the sign of ΔG_{obs}^0 changes as the unprotonated state $\text{Q}_\text{A}^- \text{Q}_\text{B}$ becomes energetically favored ($\Delta G_{\text{o}}^0 = \Delta G_{\text{H}^+}^0 - kT \cdot \ln 10 \cdot (\text{p}K_{\text{A}^-} - \text{p}K_{\text{B}^-}) = +22$ meV; see Eqn. 11).

The pH dependence of the rates k_{AB} and k_{BA}

The measurement of the observed $\text{Q}_\text{A}^- \text{Q}_\text{B} \rightleftharpoons \text{Q}_\text{A} \text{Q}_\text{B}^-$ electron transfer rate can be combined with the results of the free energy difference between these states to yield the individual forward and reverse rates, k_{AB} and k_{BA} . This analysis assumes that the free energy results are applicable on the time scale of $k_{\text{Q}_\text{A}^- \rightarrow \text{Q}_\text{A}}^{\text{obs}}$ rather than that of $k_{\text{D}^+ \rightarrow \text{D}}^{\text{obs}}$ from which the energies were derived. The rate constants k_{AB} and k_{BA} are determined from Eqn. 2 and the equilibrium constant K_{AB} :

$$K_{\text{AB}} = \frac{k_{\text{AB}}}{k_{\text{BA}}} = e^{-\Delta G_{\text{obs}}^0 / kT} \quad (15)$$

which results in:

$$k_{\text{AB}} = k_{\text{Q}_\text{A}^- \rightarrow \text{Q}_\text{A}}^{\text{obs}} \frac{e^{-\Delta G_{\text{obs}}^0 / kT}}{1 + e^{-\Delta G_{\text{obs}}^0 / kT}} \quad (16)$$

From the data in Figs. 3c and 6, the pH dependence of k_{AB} and k_{BA} was obtained, as shown in Fig. 7. The forward rate k_{AB} is constant at low pH, decreasing at high pH with a limiting slope of one decade per pH unit (i.e., $k_{\text{AB}} \propto [\text{H}^+]$). The break-

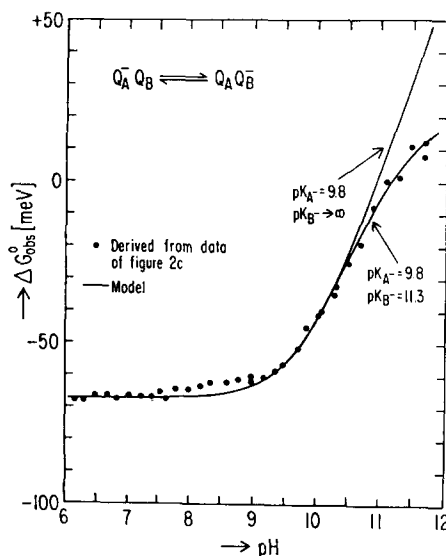


Fig. 6. The free energy difference between $\text{Q}_\text{A}^- \text{Q}_\text{B}$ and $\text{Q}_\text{A} \text{Q}_\text{B}^-$ as a function of pH. The points (●) were obtained from the kinetic data of Fig. 2c and Eqn. 14. Solid lines represent the theoretical function described by Eqn. 13 with $\Delta G_{\text{H}^+}^0 = -67$ meV and $\text{p}K_{\text{A}^-}$ and $\text{p}K_{\text{B}^-}$ as given in the figure.

point appears at a $\text{p}K$ of 9.2. The reverse rate, k_{BA} , is only weakly dependent on pH, varying approx. 20-times less than k_{AB} over the pH range investigated.

Conclusion and Discussion

The dominant charge recombination pathway between Q_B^- and D^+

We have investigated electron transfer reactions involving the quinone acceptor complex in bacterial reaction centers, focusing on the question of the charge recombination pathway between Q_B^- and D^+ . We found that the charge recombination occurs via an indirect pathway, with $\text{D}^+ \text{Q}_\text{A}^- \text{Q}_\text{B}$ serving as the intermediate state. Such a pathway was postulated by Wraight [23,5] and its existence is consistent with the recent work of Arata and Parson [4] (to be discussed later). The original, contradictory, conclusion of a direct pathway [3] was based on the finding that the decay of $\text{D}^+ \text{Q}_\text{A} \text{Q}_\text{B}^-$ was not inhibited by *o*-phen; this conclusion was subsequently invalidated by the work of Wraight and Stein [5] and Vermeglio et al. [26] who showed that *o*-phen does not bind to reaction centers in the state $\text{D}^+ \text{Q}_\text{A} \text{Q}_\text{B}^-$.

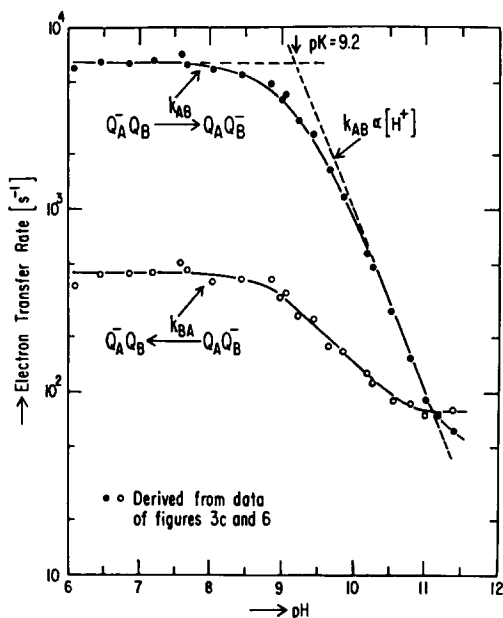


Fig. 7. The forward rate, k_{AB} , (a) and the backward rate, k_{BA} , (b) of the $Q_A^- Q_B$ to $Q_A Q_B^-$ transition as a function of pH. The points (O, ●) were obtained from the data of Figs. 3c and 6 and Eqns. 15 and 17.

The indirect pathway provides the maximum temporal stabilization of the charge on Q_B^- against recombination with D^+ . By eliminating the direct recombination pathway ($k_{BD} \rightarrow 0$), the electron must recombine via a higher lying state of the electron transfer chain, in this case $Q_A^- Q_B$. The higher the energy difference between $Q_A^- Q_B$ and $Q_A Q_B^-$, the slower the recombination rate. Thus the stabilization is paid for with a loss of free energy, the exact relation (obtained from Eqn. 14) being given by:

$$k_{D^+ \rightarrow D}^{\text{obs}} = k_{AD} / (1 + e^{-\Delta G_{\text{obs}}^0 / kT}) \quad (17)$$

Limits on the direct recombination rate, k_{BD}

The dominant charge recombination pathway was inferred from a set of independent experiments in which the following three quantities were measured: the observed charge recombination rate $k_{D^+ \rightarrow D}^{\text{obs}}$, the rate k_{AD} and the partition coefficient, α , between the states $Q_A^- Q_B$ and $Q_A Q_B^-$ (or equivalently the equilibrium constant K_{AB} or the free energy difference ΔG_{obs}^0 between these states, which

are related to α by Eqn. 14). From the discrepancy between $k_{D^+ \rightarrow D}^{\text{obs}}$ and the rate predicted from the model involving the indirect pathway (Eqn. 3), a value of k_{BD} can be determined. If no discrepancy exists a limit on k_{BD} can be obtained from an error analysis. In the present work, the main error arose from the measurement of α by the cytochrome assay, which lead to $k_{BD} \leq 0.1 \text{ s}^{-1}$. This corresponds, at high pH, to a contribution of less than or equal to 5% of the direct pathway to the observed recombination kinetics.

An alternate method of measuring α makes use of the semiquinone (i.e., Q_A^- or Q_B^-) absorption in the presence of exogenous electron donors and acceptors. This absorption exhibits damped oscillations with successive laser flashes, first observed by Vermiglio [27] and Wraight [28]. The rate of damping was shown to be governed by the equilibrium between $Q_A^- Q_B$ and $Q_A Q_B^-$ and thus serves as an assay for α [29]. The value $\alpha = 0.065 \pm 0.005$ (pH 8.0, $T = 21.5^\circ \text{C}$) was determined by this method, in good agreement with the value obtained by the cyt-*c* assay. From the uncertainty in α , the limit $k_{BD} \leq 0.1 \text{ s}^{-1}$ was deduced.

Arata and Parson [4] probed the equilibrium between $Q_A^- Q_B$ and $Q_A Q_B^-$ by comparing the relative intensities of delayed fluorescence emitted during the $D^+ Q_A Q_B^- \rightarrow D Q_A Q_B$ and $D^+ Q_A^- \rightarrow D Q_A$ charge recombinations. They found $\Delta G_{\text{obs}}^0 = -78 \pm 8 \text{ meV}$ (pH 7.8, $T = 30^\circ \text{C}$) and, from absorption measurements, $k_{AD} / k_{D^+ \rightarrow D}^{\text{obs}} = 11$. From these values the limit $k_{BD} \leq 0.3 \text{ s}^{-1}$ is calculated (Eqn. 3). Thus their results allow for a contribution of approx. 40% to the observed recombination rate by the direct pathway. These authors point out the possibility of a systematic error in ΔG_{obs}^0 introduced by the need to compare fluorescence intensities between two different samples. In contrast to their method, the cyt *c* assay as well as the previously discussed damping experiment probe the $Q_A^- Q_B \rightleftharpoons Q_A Q_B^-$ equilibrium in a single sample.

Another approach to obtain a limit on k_{BD} was to measure the temperature dependence of ΔG_{obs}^0 [10]. This dependence is expected to be linearly related to T if one assumes that the enthalpy and entropy changes, ΔH and ΔS , are assumed to be temperature independent, (i.e., $\Delta G_{\text{obs}}^0 = \Delta H - T\Delta S$). By measuring $k_{D^+ \rightarrow D}^{\text{obs}}$ and k_{AD} as a func-

tion of temperature (250 K < T < 300 K; pH 8) and using Eqn. 14 to determine ΔG_{obs}^0 , this linear relation was found to be satisfied*. In the presence of a direct pathway, Eqn. 14 becomes (for $\alpha \ll 1$):

$$\Delta G_{\text{obs}}^0 = -kT \ln \frac{k_{\text{AD}} - k_{\text{D}^+ \rightarrow \text{D}}^{\text{obs}} + k_{\text{BD}}}{k_{\text{D}^+ \rightarrow \text{D}}^{\text{obs}} - k_{\text{BD}}} \quad (18)$$

We estimated a limit on k_{BD} from an error analysis of the linear relationship between ΔG_{obs}^0 and T . Assuming k_{BD} to be temperature independent, a set of curves with different values of k_{BD} was constructed. By taking account of the statistical experimental error in the fit between ΔG_{obs}^0 and T , the limit $k_{\text{BD}} < 0.09 \text{ s}^{-1}$ was deduced. If k_{BD} is assumed to have the same temperature dependence as k_{AD} , the limiting value is lowered to $k_{\text{BD}} < 0.06 \text{ s}^{-1}$.

An inherently more precise method of determining k_{BD} would be to measure it directly, by preventing charge recombination via the intermediate state $\text{D}^+ \text{Q}_\text{A}^- \text{Q}_\text{B}$, after $\text{D}^+ \text{Q}_\text{A} \text{Q}_\text{B}^-$ was formed. This can be accomplished, in principle, by lowering the temperature. However, the electron transfer from Q_A^- to Q_B is strongly temperature dependent (i.e., enthalpy of activation $\Delta H^\ddagger = +560 \text{ meV}$ (Kleinfeld, D., Okamura, M.Y., and Feher, G., unpublished data) and the state $\text{D}^+ \text{Q}_\text{A} \text{Q}_\text{B}^-$ cannot, therefore, be produced by illuminating reaction centers that have been cooled in the dark. To overcome this problem, reaction centers were illuminated during the cooling process to trap $\text{D}^+ \text{Q}_\text{A} \text{Q}_\text{B}^-$ [30]. The observed recombination kinetics were found to be highly nonexponential, covering a spread of decay rates, $k_{\text{D}^+ \rightarrow \text{D}}^{\text{obs}}$ ranging from approx. 10^{-2} to below 10^{-5} s^{-1} ($T < 80 \text{ K}$; pH 8) [30]. Assuming that the high temperature values for ΔH and ΔS (see above) are valid with reaction centers cooled under illumination, the predicted rate for the indirect pathway is $2 \cdot 10^{-11} \text{ s}^{-1}$ (!) at 80 K (Eqn. 17 with $k_{\text{AD}} = 40 \text{ s}^{-1}$ [15,30]). This is much smaller than the measured range of rates. Thus it appears that at low temperature the direct pathway predominates.

* We determined the following values: $\Delta H = -230 \text{ meV}$ and $\Delta S = -0.55 \text{ meV} \cdot \text{K}^{-1}$ [10]. These values differ from those recently reported by Mancino et al. [48]. The origin of this discrepancy is at present not understood.

The pH dependence of ΔG_{obs}^0 and its relation to redox titrations and proton uptake

The free energy difference between the states $\text{Q}_\text{A}^- \text{Q}_\text{B}$ and $\text{Q}_\text{A} \text{Q}_\text{B}^-$ is equal to the difference in reduction-oxidation (redox) energies between the $\text{Q}_\text{A} \text{Q}_\text{B} / \text{Q}_\text{A} \text{Q}_\text{B}^-$ and $\text{Q}_\text{A} \text{Q}_\text{B} / \text{Q}_\text{A}^- \text{Q}_\text{B}$ couples. Redox titrations of Q_A performed on chromatophores [6,7] or isolated reaction centers incorporated into phospholipid vesicles [8] indicate that the midpoint potential for the $\text{Q}_\text{A} \text{Q}_\text{B} / \text{Q}_\text{A}^- \text{Q}_\text{B}$ couple is pH dependent, with a slope of approx. 60 mV per pH unit, up to a $\text{p}K_{\text{A}^-}$ of approx. 9.8; this is the same $\text{p}K_{\text{A}^-}$ value found from the free energy results (Fig. 6). Redox titrations of Q_B have been performed only at a few pH values in chromatophores [7]. They indicate that the midpoint potential for the $\text{Q}_\text{A} \text{Q}_\text{B} / \text{Q}_\text{A} \text{Q}_\text{B}^-$ couple is also pH dependent, but a reliable value for $\text{p}K_{\text{B}^-}$ has so far not been determined.

The pH dependence of the redox couples $\text{Q}_\text{A} \text{Q}_\text{B} / \text{Q}_\text{A}^- \text{Q}_\text{B}$ and $\text{Q}_\text{A} \text{Q}_\text{B} / \text{Q}_\text{A} \text{Q}_\text{B}^-$ that yields the free energy difference found between the states $\text{Q}_\text{A}^- \text{Q}_\text{B}$ and $\text{Q}_\text{A} \text{Q}_\text{B}^-$ (see Fig. 6) are shown in Fig. 8. The curves were constructed using the relation (e.g., see Ref. 31):

$$G_{\text{Q}_\text{A} \text{Q}_\text{B} / \text{Q}_\text{A}^- \text{Q}_\text{B}}^{\text{redox}} = G_{(\text{Q}_\text{A}^- \text{Q}_\text{B})\text{H}^+}^0 - kT \ln \frac{1 + 10^{\text{pH} - \text{p}K_{\text{A}^-}}}{1 + 10^{\text{pH} - \text{p}K_0}} \quad (19)$$

with an equivalent expression for $G_{\text{Q}_\text{A} \text{Q}_\text{B} / \text{Q}_\text{A} \text{Q}_\text{B}^-}^{\text{redox}}$. $\text{p}K_0$ describes protonation of the neutral state $\text{Q}_\text{A} \text{Q}_\text{B}$. Its value is less than 5 [6,8] and therefore does not enter into the analysis. At low pH the free energy difference ΔG_{obs}^0 equals $\Delta G_{\text{H}^+}^0$ (see Eqn. 13) and is pH independent as both $\text{Q}_\text{A}^- \text{Q}_\text{B}$ and $\text{Q}_\text{A} \text{Q}_\text{B}^-$ associate with a proton. Similarly, at high pH ΔG_{obs}^0 equals ΔG_0^0 and is again pH independent as both states remain unprotonated. The pH dependent transition region occurs between $\text{p}K_{\text{A}^-} = 9.8$ and $\text{p}K_{\text{B}^-} = 11.3$.

The results of Fig. 8 show that $\text{Q}_\text{A} \text{Q}_\text{B}^-$ is stabilized relative to $\text{Q}_\text{A}^- \text{Q}_\text{B}$ under physiological conditions (pH < 9). At high pH, $\text{Q}_\text{A} \text{Q}_\text{B}^-$ is energetically less stable than $\text{Q}_\text{A}^- \text{Q}_\text{B}$. The stabilization of $\text{Q}_\text{A} \text{Q}_\text{B}^-$ at low pH results from the interaction with a proton which is stronger for Q_B^- than for Q_A^- **.

** The stabilization energy is given by (see Eqn. 11) $\Delta G_{\text{H}^+}^0 - \Delta G_0^0 = -kT \ln 10 \cdot (\text{p}K_{\text{B}^-} - \text{p}K_{\text{A}^-}) = -88 \text{ meV}$ at $T = 21^\circ \text{C}$.

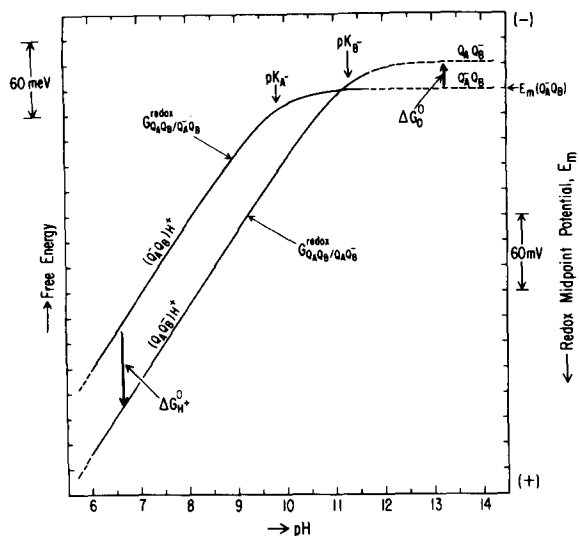


Fig. 8. The pH dependence of the redox free energy (or equivalently the redox midpoint potential) of the $Q_A Q_B / Q_A^- Q_B^-$ and $Q_A Q_B / Q_A Q_B^-$ couples. The curves were constructed by using Eqn. 19 with $pK_A^- = 9.8$, $pK_0 \ll 6$ and $T = 21.5^\circ\text{C}$, and the equivalent expression for $G_{Q_A Q_B / Q_A Q_B^-}^{\text{redox}}$ with $pK_B^- = 11.3$. The difference between the two curves was established from a knowledge of the limiting values of ΔG_{obs}^0 at low or high pH (i.e., $\Delta G_{\text{H}^+}^0 = -67$ meV, $\Delta G_{\text{O}}^0 = +22$ meV) and represents the energy difference between the states $Q_A^- Q_B$ and $Q_A Q_B^-$, as shown in Fig. 6. The dashed part of the curves at high pH is an extrapolation beyond the range of the free-energy data. The midpoint potential for the unprotonated $Q_A Q_B / Q_A^- Q_B^-$ couple, $E_m(Q_A Q_B)$, was found by redox titrations to be -180 mV (vs. standard hydrogen electrode) for chromatophores [6,7] and approx. -120 mV for reaction centers reconstituted in phospholipid vesicles [8].

It is this preferential interaction that provides the driving force and necessary asymmetry between Q_A^- and Q_B^- to allow the electron transfer to occur in the forward direction.

The pH dependence of the redox couples shown in Fig. 8 predicts an uptake of one proton per reaction center when the charge separation is formed below pH 9.8. Furthermore, since the pH dependence of ΔG_{obs}^0 was obtained from kinetic measurements, the proton uptake must occur rapidly compared to $k_{\text{D}^+ \rightarrow \text{D}}^{\text{obs}}$ (i.e., faster than 0.1 s). The experimental results on the stoichiometry of proton uptake are controversial [23,32,33]. Cogdell et al. [32] found a 1:1 stoichiometry in isolated RC reaction centers following a single flash (pH 7.5). Wraight [23], on the other hand, reported a strongly pH-dependent proton uptake that de-

creased to zero at a pH of approx. 6. The latter result contradicts both the redox and free energy measurements. This discrepancy may be connected with the kinetics of protonation. For example the proton may be donated by surface charges on the reaction center or by the detergent (LDAO) in a manner similar to that proposed for phospholipid membranes [34]; the proton donor may then equilibrate only slowly with the outside solution. The use of reaction center isolated with other detergents (e.g., octyl- β -glucoside) may help to resolve this problem.

The pH dependence of the electron transfer rate between Q_A and Q_B

The electron transfer rate from $Q_A^- Q_B$ to $Q_A Q_B^-$ was first determined at pH 7.5 by Vermeglio and Clayton [22]. The pH dependence of this rate was subsequently measured by Wraight [23] and Vermeglio [24]. Both investigators found that $k_{Q_A^- \rightarrow Q_A}^{\text{obs}}$ was approximately proportional to $[\text{H}^+]^{0.3}$ in the pH range from approx. 6 to approx. 10. These findings are in contradiction with those reported in this work (see Fig. 3c). We duplicated the conditions used by Wraight and Vermeglio, but were unable to reproduce their results. The origin of this discrepancy is at present not understood.

The pH dependence of the observed transfer rate is dominated by the pH dependence of the forward rate k_{AB} (see Fig. 7) and can be understood in the light of the previous discussion on ΔG_{obs}^0 . The electron transfer from Q_A^- to Q_B is energetically favorable only if $Q_A^- Q_B$ is protonated (see Fig. 8). Thus at high pH, the electron transfer becomes unfavorable and k_{AB} decreases. If protonation of $Q_A^- Q_B$ occurs rapidly compared to k_{AB} , the pK obtained from the kinetic measurements (Fig. 7) should be the same (i.e., 9.8) as measured under quasiequilibrium conditions (Fig. 6). The observed pK is slightly lower (9.2), indicating that the proton uptake time may be the rate-limiting step.

The location of the proton-binding site

Optical spectra of Q_A^- and Q_B^- [22] near neutral pH resemble those of the unprotonated species of UQ^- in solution [35,36]. Similarly, the line width of the EPR spectrum of Q_A^- in iron free reaction

centers [37] was found to be characteristic of the unprotonated form [38]. How can these findings be reconciled with the free energy results, which predict an association of a proton with the quinones? If the proton binds to a nearby amino acid residue rather than directly to Q_A^- or Q_B^- , the interaction of the proton with the quinones will be greatly reduced; consequently, the presence of the proton will have little effect on the optical and EPR spectra. Models for the protonation sites embodying these ideas have been proposed by Wraight [23,39].

An approach taken to probe for the presence of the proton utilized the sensitivity of the recombination rate k_{AD} to small perturbations in the energy of Q_A^- . This sensitivity is observed with reaction centers in which anthraquinone is substituted for the native UQ in the Q_A binding site [40,41]. The recombination rate in this system was found to be pH dependent with a pK of 9.8 [42]. This result was interpreted as being caused by a proton binding in the vicinity of Q_A^- .

The M protein subunit of the reaction center is believed to contain the binding sites for both Q_A [43] and Q_B [44]; it is therefore likely to contain also the proton binding site. The amino acid sequence of this subunit [45] includes a number of basic residues (e.g., Arg. 164) that are potential candidates for the site. Further studies involving chemical and/or genetic modification of the reaction center protein should help characterize the proton binding site.

Acknowledgements

We thank E. Abresch for the preparation of the reaction centers and D. Fredkin and J. Allen for helpful discussions. The work was supported by the National Science Foundation (PCM 82-02811) and the National Institute of Health (GM 13191).

Appendix. Rate equations governing electron transfer kinetics after a single flash

The rate equations describing the electron transfer kinetics in reaction centers for the scheme depicted in Fig. 1 are given by:

$$\begin{aligned} & \frac{d}{dt} \begin{pmatrix} [DQ_A Q_B] \\ [D^+ Q_A^- Q_B] \\ [D^+ Q_A Q_B^-] \end{pmatrix}_t \\ &= \begin{pmatrix} -k_L & k_{AD} & k_{BD} \\ k_L & -(k_{AD} + k_{AB}) & k_{BA} \\ 0 & k_{AB} & -(k_{BD} + k_{BA}) \end{pmatrix} \\ & \cdot \begin{pmatrix} [DQ_A Q_B] \\ [D^+ Q_A^- Q_B] \\ [D^+ Q_A Q_B^-] \end{pmatrix} \end{aligned} \quad (A-1)$$

The steady state solutions of Eqn. A-1 are:

$$\begin{aligned} & \begin{pmatrix} [DQ_A Q_B] \\ [D^+ Q_A^- Q_B] \\ [D^+ Q_A Q_B^-] \end{pmatrix}_{t \rightarrow \infty} \\ &= \frac{N_0}{k_L(k_{BD} + k_{AB} + k_{BA}) + k_{AD}k_{BA} + k_{BD}(k_{AD} + k_{AB})} \\ & \times \begin{pmatrix} k_{AD}k_{BA} + k_{BD}(k_{AD} + k_{AB}) \\ k_L(k_{BD} + k_{BA}) \\ k_L k_{AB} \end{pmatrix} \end{aligned} \quad (A-2)$$

where $N_0 = [DQ_A Q_B]_t + [D^+ Q_A^- Q_B]_t + [D^+ Q_A Q_B^-]_t$ is the total concentration of reaction centers.

The general time-dependent solution is algebraically unwieldy; we shall consider therefore only the solutions after a short (i.e., faster than the non-light-induced rates) saturating (i.e., $\int k_L(t) dt \gg 1$) flash. This corresponds to the initial conditions $[DQ_A Q_B]_0 = 0$, $[D^+ Q_A^- Q_B]_0 = N_0$, $[D^+ Q_A Q_B^-]_0 = 0$, and $k_L = 0$. The two observed rates are given by:

$$\begin{aligned} k_{1,2} &= \frac{(k_{AB} + k_{BA}) + k_{AD} + k_{BD}}{2} \\ & \pm \left\{ \left(\frac{(k_{AB} + k_{BA}) + k_{AD} + k_{BD}}{2} \right)^2 \right. \\ & \left. - (k_{AB} + k_{BA})(\alpha k_{AD} + (1 - \alpha)k_{BD}) - k_{AD}k_{BD} \right\}^{-\frac{1}{2}} \end{aligned} \quad (A-3)$$

with:

$$\alpha \equiv \frac{k_{BA}}{k_{AB} + k_{BA}} \quad (\text{A-4})$$

We present the time-dependent solution for the various reaction centers species for two limiting cases of interest: one applicable for reaction centers at room temperature (Case I), the other is encountered when the temperature is lowered (Case II). We keep second-order terms in the observed rates but only leading terms in the coefficients.

Case I. $k_{AB} + k_{BA} \gg k_{AD}$ and $k_{AB} + k_{BA} \gg k_{BD}$

$$[\text{DQ}_A\text{Q}_B]_t = N_0 - N_0(1-\alpha) \frac{k_{AD} - k_{BD}}{k_{AB} + k_{BA}} \exp(-k_{Q_A^- \rightarrow Q_A} \cdot t) - N_0 \exp(-k_{D^+ \rightarrow D} \cdot t) \quad (\text{A-5a})$$

$$[\text{D}^+ \text{Q}_A^- \text{Q}_B]_t = N_0(1-\alpha) \exp(-k_{Q_A^- \rightarrow Q_A} \cdot t) + N_0 \alpha \exp(-k_{D^+ \rightarrow D} \cdot t) \quad (\text{A-5b})$$

$$[\text{D}^+ \text{Q}_A \text{Q}_B^-]_t = -N_0(1-\alpha) \exp(-k_{Q_A^- \rightarrow Q_A} \cdot t) + N_0(1-\alpha) \exp(-k_{D^+ \rightarrow D} \cdot t) \quad (\text{A-5c})$$

where:

$$k_{Q_A^- \rightarrow Q_A} = (k_{AB} + k_{BA}) \left(1 + \frac{(1-\alpha)k_{AD} + \alpha k_{BD}}{(k_{AB} + k_{BA})} \right) \quad (\text{A-6})$$

and:

$$k_{D^+ \rightarrow D} = [\alpha k_{AD} + (1-\alpha)k_{BD}] \left(1 - \frac{(1-\alpha)k_{AD} + \alpha k_{BD}}{(k_{AB} + k_{BA})} \right) \quad (\text{A-7})$$

For $t \gg (k_{Q_A^- \rightarrow Q_A})^{-1}$ α can be written as:

$$\alpha = \frac{[\text{D}^+ \text{Q}_A^- \text{Q}_B]_t}{[\text{D}^+ \text{Q}_A^- \text{Q}_B]_t + [\text{D}^+ \text{Q}_A \text{Q}_B^-]_t} \quad (\text{A-8})$$

The rate $k_{Q_A^- \rightarrow Q_A}$ is essentially the $\text{D}^+ \text{Q}_A^- \text{Q}_B \rightleftharpoons \text{D}^+ \text{Q}_A \text{Q}_B^-$ electron-transfer rate and the rate $k_{D^+ \rightarrow D}$ is essentially the charge recombination rate of $\text{D}^+ \text{Q}_A \text{Q}_B^-$, which dominates the observed recovery of DQ_AQ_B . In this approximation, $\text{D}^+ \text{Q}_A^- \text{Q}_B$ rapidly decays to its equilibrium value, αN_0 , with rate $k_{Q_A^- \rightarrow Q_A}$, and then decays to zero with rate $k_{D^+ \rightarrow D}$. Similarly, $\text{D}^+ \text{Q}_A \text{Q}_B^-$ rapidly builds up to its equilibrium value, $N_0(1-\alpha)$, with

rate $k_{Q_A^- \rightarrow Q_A}$, and then decays with rate $k_{D^+ \rightarrow D}$.
Case II. $k_{AD}, k_{AB} \gg k_{BA}, k_{BD}$

$$[\text{DQ}_A\text{Q}_B]_t = N_0 - N_0 \frac{k_{AD}}{k_{AD} + k_{AB}} \exp(-k_{Q_A^- \rightarrow Q_A} \cdot t) - N_0 \frac{k_{AB}}{k_{AD} + k_{AB}} \exp(-k_{D^+ \rightarrow D} \cdot t) \quad (\text{A-9a})$$

$$[\text{D}^+ \text{Q}_A^- \text{Q}_B]_t = N_0 \exp(-k_{Q_A^- \rightarrow Q_A} \cdot t) + N_0 \frac{k_{BA}}{k_{AD} + k_{AB}} \frac{k_{AB}}{k_{AD} + k_{AB}} \times \exp(-k_{D^+ \rightarrow D} \cdot t) \quad (\text{A-9b})$$

$$[\text{D}^+ \text{Q}_A \text{Q}_B^-]_t = -N_0 \frac{k_{AB}}{k_{AD} + k_{AB}} \exp(-k_{Q_A^- \rightarrow Q_A} \cdot t) + N_0 \left(\frac{k_{AB}}{k_{AD} + k_{AB}} \right) \exp(-k_{D^+ \rightarrow D} \cdot t) \quad (\text{A-9c})$$

with:

$$k_{Q_A^- \rightarrow Q_A} = (k_{AD} + k_{AB}) \left\{ 1 + \frac{k_{BA}}{k_{AD} + k_{AB}} \left(1 + \frac{k_{AD}}{k_{AD} + k_{AB}} \right) \right\} \quad (\text{A-10})$$

and:

$$k_{D^+ \rightarrow D} = \left(\frac{k_{BA}}{k_{AD} + k_{AB}} k_{AD} + k_{BD} \right) \left(1 - \frac{k_{BA} + k_{BD}}{k_{AD} + k_{AB}} \right) \quad (\text{A-11})$$

For this case, $k_{Q_A^- \rightarrow Q_A}$ represents the rate at which electrons leave Q_A^- form either DQ_AQ_B or $\text{D}^+ \text{Q}_A \text{Q}_B^-$, while $k_{D^+ \rightarrow D}$ is the charge recombination rate of $\text{D}^+ \text{Q}_A \text{Q}_B^-$. Note that the indirect pathway component for this charge recombination can no longer be written as αk_{AD} . The recovery rate of DQ_AQ_B is biphasic with the two rate constants given by Eqns. A-10 and A-11. The above solutions form the basis of the method of Chamorovsky et al. [46] for measuring k_{AB} when k_{AB} and k_{AD} are of the same order or magnitude. The ratio of amplitudes of the component with rate $k_{Q_A^- \rightarrow Q_A}$ to the component with rate $k_{D^+ \rightarrow D}$ is k_{AD}/k_{AB} , independent of the charge recombina-

tion pathway of $D^+Q_AQ_B^-$. The rate k_{AD} can be determined from a separate measurement on reaction centers with one quinone or reaction centers in the presence of *o*-phen; alternately, $k_{AD} + k_{AB}$ can be found from $k_{Q_A^- \rightarrow Q_A^*}$. Thus k_{AB} is determined.

References

- 1 Feher, G. and Okamura, M.Y. (1978) in *The Photosynthetic Bacteria* (Clayton, R.K. and Sistrom, W.R., eds.), pp. 349–386, Plenum Press, New York
- 2 Parson, W.W. and Ke, B. (1982) in *Photosynthesis. Energy Conversion by Plants and Bacteria* (Govindjee, ed.), pp. 331–385, Academic Press, New York
- 3 Blankenship, R.E. and Parson, W.W. (1979) *Biochim. Biophys. Acta* 545, 429–444
- 4 Arata, H. and Parson, W.W. (1981) *Biochim. Biophys. Acta* 638, 201–209
- 5 Wraight, C.A. and Stein R.R. (1980) *FEBS Lett.* 113, 73–77
- 6 Prince, R.C. and Dutton, P.L. (1976) *Arch. Biochim. Biophys.* 172, 329–334
- 7 Rutherford, A.W. and Evans, M.C.W. (1980) *FEBS Lett.* 110, 257–261
- 8 Wraight, C.A. (1981) *Isr. J. Chem.* 21, 348–354
- 9 Kleinfeld, D., Okamura, M.Y. and Feher, G. (1982) *Biophys. J. (Abstr.)* 37, 110a
- 10 Kleinfeld, D., Okamura, M.Y. and Feher, G. (1982) *Biophys. J. (Abstr.)* 37, 110a
- 11 Bartsch, R.G. (1978) in *The Photosynthetic Bacteria* (Clayton, R.K. and Sistrom, W.R., eds.), pp. 249–279, Plenum Press, New York
- 12 Okamura, M.Y., Isaacson, R.A. and Feher, G. (1975) *Proc. Natl. Acad. Sci. USA* 72, 3491–3495
- 13 Butler, W.F., Johnston, D.C., Shore, H.B., Fredkin, D.R., Okamura, M.Y. and Feher, G. (1980) *Biophys. J.* 32, 967–992
- 14 Okamura, M.Y., Debus, R.J., Kleinfeld, D. and Feher, G. (1982) in *Function of Quinones in Energy-Conserving Systems* (Trumpower, B.L., ed.), pp. 299–317, Academic Press, New York
- 15 McElroy, J.D., Mauzerall, D.C. and Feher, G. (1974) *Biochim. Biophys. Acta* 333, 261–278
- 16 Parson, W.W. (1969) *Biochim. Biophys. Acta* 189, 384–396
- 17 Case, G.D. and Parson, W.W. (1971) *Biochim. Biophys. Acta* 253, 187–202
- 18 Parson, W.W., Clayton, R.K. and Cogdell, D.J. (1975) *Biochim. Biophys. Acta* 387, 265–278
- 19 Ke, B., Chaney, T.H. and Reed, D.W. (1970) *Biochim. Biophys. Acta* 216, 373–383
- 20 Prince, R.C., Cogdell, R.J. and Crofts, A.R. (1974) *Biochim. Biophys. Acta* 347, 1–13
- 21 Rosen, D., Okamura, M.Y. and Feher, G. (1979) *Biophys. J. (Abstr.)* 25, 204a
- 22 Vermeglio, A. and Clayton, R.K. (1977) *Biochim. Biophys. Acta* 461, 159–165
- 23 Wraight, C.A. (1979) *Biochim. Biophys. Acta* 548, 309–327
- 24 Vermeglio, A. (1982) in *Function of Quinones in Energy-Conserving Systems* (Trumpower, R.L., ed.), pp. 169–180, Academic Press, New York
- 25 Duysens, L.N.M., Huiskamp, W.J., Vos, J.J. and Van der Hart, J.M. (1956) *Biochim. Biophys. Acta* 19, 188–190
- 26 Vermeglio, A., Martinet, T. and Clayton, R.K. (1980) *Proc. Natl. Acad. Sci. USA* 77, 1809–1813
- 27 Vermeglio, A. (1977) *Biochim. Biophys. Acta* 459, 516–524
- 28 Wraight, C.A. (1977) *Biochim. Biophys. Acta* 459, 525–531
- 29 Kleinfeld, D., Abresch, E.C., Okamura, M.Y. and Feher, G. (1984) *Biochim. Biophys. Acta* 765, 406–409
- 30 Kleinfeld, D., Okamura, M.Y. and Feher, G. (1984) *Biochemistry*, in the press
- 31 Dutton, P.L. (1978) *Methods Enzymol.* 54, 411–435
- 32 Cogdell, R.J., Prince, R.C. and Crofts, A.R. (1973) *FEBS Lett.* 35, 204–208
- 33 Wraight, C.A., Cogdell, R.J. and Clayton, R.K. (1975) *Biochim. Biophys. Acta* 396, 242–249
- 34 Haines, T.H. (1983) *Proc. Natl. Acad. Sci. USA* 80, 160–164
- 35 Morrison, L.E., Schelhorn, J.E., Cotton, T.M., Bering, C.L. and Loach, P.A. (1982) in *Function of Quinones in Energy-Conserving Systems* (Trumpower, B.L., ed.), pp. 35–58, Academic Press, New York
- 36 Bensasson, R. and Land, E.J. (1973) *Biochim. Biophys. Acta* 325, 175–181
- 37 Feher, G., Okamura, M.Y. and McElroy, J.D. (1972) *Biochim. Biophys. Acta* 267, 222–226
- 38 Hales, B.J. and Case, E.E. (1981) *Biochim. Biophys. Acta* 637, 291–302
- 39 Wraight, C.A. (1982) in *Function of Quinones in Energy-Conserving Systems* (Trumpower, B.L., ed.), pp. 181–197, Academic Press, New York
- 40 Gunner, M.R., Tiede, D.M., Prince, R.C. and Dutton, P.L. (1982) in *Function of Quinones in Energy-Conserving Systems* (Trumpower, B.L., ed.), pp. 265–269, Academic Press, New York
- 41 Gopher, A., Blatt, Y., Okamura, M.Y., Feher, G. and Montal, M. (1983) *Biophys. J. (Abstr.)* 41, 121a
- 42 Kleinfeld, D., Okamura, M.Y. and Feher, G. (1984) *Biophys. J. (Abstr.)* 45, 256a
- 43 Marinetti, T.D., Okamura, M.Y. and Feher, G. (1979) *Biochemistry* 18, 3126–3133
- 44 Debus, R.J., Valkirs, G.E., Okamura, M.Y. and Feher, G. (1982) *Biochim. Biophys. Acta* 682, 500–503
- 45 Williams, J.C., Steiner, L.A., Ogden, R.C., Simon, M.I. and Feher, G. (1983) *Proc. Natl. Acad. Sci. USA* 80, 6505–6509
- 46 Chamorovsky, S.K., Remennikov, S.M., Kononenko, A.A., Venediktov, P.S. and Rubin, A.B. (1976) *Biochim. Biophys. Acta* 430, 62–70
- 47 Mancino, L.J., Dean, D.P. and Blankenship, R.E. (1984) *Biochim. Biophys. Acta* 764, 46–54
- 48 Overfield, R.E., Wraight, C.A. and Devault, D. (1979) *FEBS Lett.* 105, 137–142